




# Utilization of Host Polyamines in Alternatively Activated Macrophages Promotes Chronic Infection by *Brucella abortus*

Tobias Kerrinnes,<sup>a,b</sup> Maria G. Winter,<sup>c</sup> Briana M. Young,<sup>a</sup> Vladimir E. Diaz-Ochoa,<sup>a</sup>  Sebastian E. Winter,<sup>c</sup>  Renée M. Tsolis<sup>a</sup>

<sup>a</sup>Department of Medical Microbiology and Immunology, School of Medicine, University of California, Davis, Davis, California, USA

<sup>b</sup>Helmholtz-Zentrum für Infektionsforschung, Braunschweig, Germany

<sup>c</sup>Department of Microbiology, University of Texas Southwestern Medical Center, Dallas, Texas, USA

**ABSTRACT** Treatment of intracellular bacterial pathogens with antibiotic therapy often requires a long course of multiple drugs. A barrier to developing strategies that enhance antibiotic efficacy against these pathogens is our poor understanding of the intracellular nutritional environment that maintains bacterial persistence. The intracellular pathogen *Brucella abortus* survives and replicates preferentially in alternatively activated macrophages (AAMs); however, knowledge of the metabolic adaptations promoting exploitation of this niche is limited. Here we show that one mechanism promoting enhanced survival in AAMs is a shift in macrophage arginine utilization from production of nitric oxide (NO) to biosynthesis of polyamines, induced by interleukin 4 (IL-4)/IL-13 treatment. Production of polyamines by infected AAMs promoted both intracellular survival of *B. abortus* and chronic infection in mice, as inhibition of macrophage polyamine synthesis or inactivation of the putative putrescine transporter encoded by *potIHGF* reduced both intracellular survival in AAMs and persistence in mice. These results demonstrate that increased intracellular availability of polyamines induced by arginase-1 expression in IL-4/IL-13-induced AAMs promotes chronic persistence of *B. abortus* within this niche and suggest that targeting of this pathway may aid in eradicating chronic infection.

**KEYWORDS** nitrogen metabolism, putrescine

Several intracellular pathogens that cause chronic infections can establish persistence within the mononuclear phagocyte system, including *Salmonella enterica* serovar Typhi (*S. Typhi*), *Mycobacterium* species, *Leishmania*, and *Brucella* species (1–4). Within infected tissues, these pathogens can be found in association with different populations of macrophages (5–7). Like other immune cells, macrophages are recognized to adopt a spectrum of different functional states that are influenced by the immune microenvironment (reviewed in references 8 and 9). Functional states that can be modeled *in vitro* include activation by gamma interferon (IFN- $\gamma$ ), which induces the classically activated macrophage (CAM; also known as M1) phenotype, characterized by production of nitric oxide (NO) and inflammatory cytokines such as tumor necrosis factor alpha (TNF- $\alpha$ ) and interleukin 6 (IL-6). During inflammation *in vivo*, cells with a similar phenotype can arise from Ly6C<sup>high</sup> inflammatory monocytes that leave the bone marrow in a C-C chemokine receptor type 2 (CCR2)-dependent manner (10). In contrast, *in vitro*, the Th2 cytokines IL-4 and IL-13 activate signal transducer and activator of transcription 6 (STAT6) to promote the development of alternatively activated macrophages (AAMs), which play important roles in allergic inflammation, helminth infection, and tissue repair (11–13).

In addition to roles in inflammation and immunity, these different macrophage populations differ in their metabolic capacity (reviewed in reference 14), with IFN- $\gamma$  activation

Received 28 June 2017 Returned for modification 13 July 2017 Accepted 29 November 2017

Accepted manuscript posted online 4 December 2017

**Citation** Kerrinnes T, Winter MG, Young BM, Diaz-Ochoa VE, Winter SE, Tsolis RM. 2018. Utilization of host polyamines in alternatively activated macrophages promotes chronic infection by *Brucella abortus*. *Infect Immun* 86:e00458-17. <https://doi.org/10.1128/IAI.00458-17>.

**Editor** Guy H. Palmer, Washington State University

**Copyright** © 2018 American Society for Microbiology. All Rights Reserved.

Address correspondence to Renée M. Tsolis, [rmtsolis@ucdavis.edu](mailto:rmtsolis@ucdavis.edu).

inducing a glycolytic energy metabolism while IL-4/IL-13 treatment promotes a shift to mitochondrial  $\beta$ -oxidation that is dependent on peroxisome proliferator-activated receptors (PPARs [15]). The resulting increase in intracellular glucose availability enhances intracellular replication of both *S. Typhi* and *Brucella abortus* (16, 17).

A second metabolic program with divergent functions in distinct macrophage subsets is arginine consumption. In IFN- $\gamma$ -activated macrophages, arginine serves as a substrate of inducible nitric oxide synthase (iNOS), which converts it to NO and L-citrulline. In contrast, IL-4/IL-13 exposure induces expression of macrophage arginase-1 (18), which catalyzes the first step in biosynthesis of the polyamines putrescine, spermine, and spermidine. An IL-4/IL-13-mediated shift in macrophage arginine metabolism promotes infection with *Leishmania* spp.; however, the mechanism by which this growth promotion occurs is unclear (19).

*Brucella abortus* causes chronic intracellular infections in humans and animals (4). In mouse infection models, bacteria are found in association with phagocytic cells, most prominently macrophages, in which a subset of *B. abortus* can evade killing in phagolysosomes. These bacteria replicate within an endoplasmic reticulum-associated compartment and can interact subsequently with a modified autophagy pathway to promote their cell-to-cell spread (20, 21). While bacteria can be found in association with macrophages having characteristics of both classical (IFN- $\gamma$ ) and alternative (IL-4/IL-13 or IL-10) activation during the initial stages of infection in mice, as infection progresses bacteria are found preferentially within phagocytes that exhibit gene expression profiles characteristic of alternative activation states (16). Interestingly, the *B. abortus* genome encodes transporters for ornithine and polyamines, the products of macrophage arginase-1, suggesting that arginase-1 expression may provide nutrients for growth of *B. abortus* within arginase-expressing macrophages. The goal of this study was to determine whether activation of the arginase-1 pathway in AAMs contributes to the ability of this cell population to serve as a site for chronic infection with *B. abortus*.

## RESULTS

***B. abortus* relies on putrescine uptake to boost bacterial growth in vitro.** Polyamines such as putrescine are essential secondary metabolites that can be linked directly to basic cellular homeostasis in eukaryotic as well as prokaryotic cells. Interestingly, a survey of the *B. abortus* 2308 genome sequence (22) showed that homologs of the *S. Typhimurium* and *Escherichia coli* genes required for synthesis of putrescine from L-arginine and L-ornithine appear to be absent (Fig. 1A). However, the *B. abortus* genome does encode homologs of *E. coli* PatA, PatD, and PuuA, -B, -C, and -D, which mediate the catabolism of putrescine to succinate via  $\gamma$ -aminobutyraldehyde (GABA) (Fig. 1A) (23). Therefore, we investigated whether putrescine could be used as a nutrient source during *B. abortus* growth *in vitro*. For this purpose, we reformulated a chemically defined medium with and without putrescine based on the composition of Ham's F-12K (Kaighn's) medium from Invitrogen (USA). *B. abortus* 2308 exhibited modest growth over 24 h in medium containing putrescine; however, in the absence of putrescine no growth was observed (Fig. 1B; see also Fig. S1A in the supplemental material). To determine the contribution of putrescine uptake to the growth of *B. abortus* in this medium, we inactivated the *potIHGF* genes (BAB1\_1624 to BAB1\_1628; strain TOK13), which based on similarity to the *pot* genes in *E. coli* (24) were predicted to encode a putrescine-specific ATP binding cassette transporter. The *potIHGF* mutant grew normally in tryptic soy broth (TSB) but exhibited no growth in putrescine-containing F12/K medium (Fig. 1B and S1B). These results suggest that *B. abortus* PotIHGF contributes to growth in the presence of putrescine.

***B. abortus* persists in BALB/c mice within CD11b<sup>+</sup> cells exhibiting features of alternate macrophage activation.** Our previous work showed that AAMs are a preferred replicative niche of *B. abortus* during chronic infections in C57BL/6J mice (16). However, for the current study, C57BL/6J mice proved not to be suitable, as this mouse strain is deficient for expression of the arginine transporter solute carrier family 7, member 2 (Slc7a2), which provides the substrate for arginase 1 during alternative

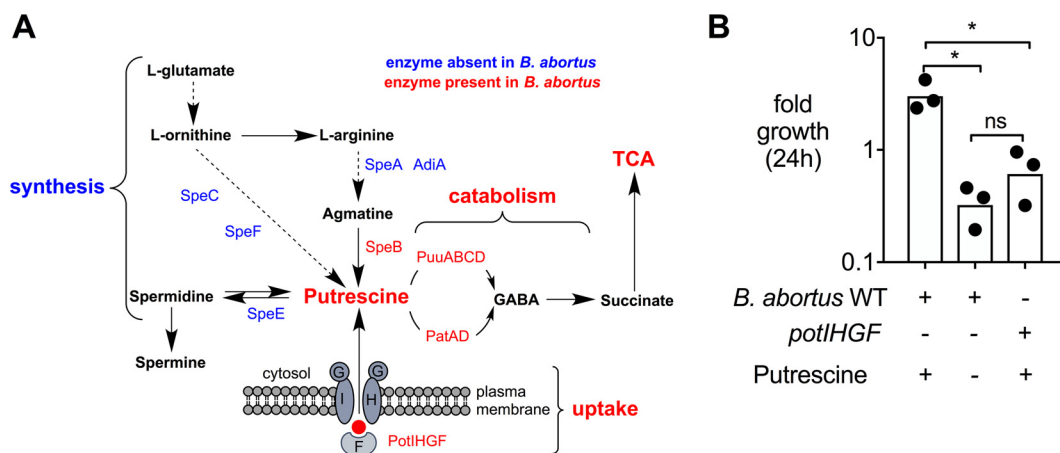


**FIG 1** Putrescine is an essential nutrient source during *B. abortus* growth *in vitro*. (A) Schematic representation of differences in polyamine synthesis between *S. Typhimurium* and *B. abortus* based on Kusano and Suzuki (44) and the most-recent genomic and metabolomic data available in the MetaCyc/BioCyc (45) and KEGG (46) databases. (B) Fold growth of *B. abortus* 2308 (wild type [WT]) in modified F12/k medium with and without putrescine as well as the *potIHGF* mutant (TOK13) at 24 h postinoculation. The inoculum was  $0.5 \times 10^5$  CFU/ml. Bars represent geometric means, and circles represent results of independent replicates. The statistical significance of differences between groups was determined using a one-way ANOVA with the Sidak multiple-comparison test. Asterisks denote statistically significant differences between groups ( $P < 0.05$ ); ns, not significant.

activation of macrophages (25). Therefore, we used BALB/c mice for these studies. Since *Il12p40*<sup>-/-</sup> mice on the BALB/c background have been shown to harbor *Brucella* predominantly within the CD11c<sup>+</sup> phagocyte subset (26), we first determined whether wild-type BALB/c mice harbor *B. abortus* within macrophages. To this end, we inoculated mice via the intraperitoneal (i.p.) route and recovered *B. abortus* from spleens at 9 and 30 days postinfection (Fig. 2). Spleens of mice were highly colonized at both time points (Fig. 2A). Enrichment of the CD11b<sup>+</sup> population by immunomagnetic separation and plating of the CD11b<sup>+</sup> cell-enriched and -depleted fractions revealed that while *B. abortus* could be isolated from both cellular subsets, greater numbers of bacteria were associated with the macrophage-containing CD11b<sup>+</sup> fraction at both time points (Fig. 2B). Characterization of gene expression profiles revealed that compared to uninfected mice, the macrophage-containing CD11b<sup>+</sup> splenocyte fraction from infected mice expressed higher levels of *Arg1*, encoding arginase, *Ym1*, encoding chitinase, and *Slc7a2*, encoding the arginine amino acid transporter, which are markers of alternate macrophage activation (Fig. 2C). In contrast to what was seen in C57BL/6 mice, expression of AAM markers in BALB/c mice at day 9 postinfection is higher, which could be attributed to a reduced production of gamma interferon in *B. abortus*-infected BALB/c mice compared to C57BL/6 mice (data not shown). These results show that in BALB/c mice *B. abortus* persists within macrophages in the spleen and that this cell population exhibits features of AAMs.

**Arginase-1 activity contributes to chronic infection by *B. abortus*.** Our finding that *Arg1* is upregulated in murine macrophages during *B. abortus* infection raised the question whether arginase activity promotes bacterial persistence. To determine the contribution of arginase-1 to survival of *B. abortus* in the mononuclear phagocyte system, we blocked arginase-1 activity in infected mice using the inhibitor *N*(omega)-hydroxy-nor-L-arginine (nor-NOHA) (27). For these experiments, mice inoculated via the i.p. route with *B. abortus* were treated daily with vehicle or nor-NOHA for 6 days before necropsy at either 9 days or 30 days postinfection (Fig. 3A and B). Treatment with nor-NOHA reduced the splenic bacterial burden 2-fold during the acute phase of infection (9 days) compared to the vehicle treatment (Fig. 3B). This effect was greater during chronic infection (30 days), when 6-fold-fewer bacteria were recovered from the nor-NOHA-treated group.

The reduction in *B. abortus* infection levels by inhibition of arginase-1 raised the question of which downstream products *B. abortus* might utilize for its intracellular

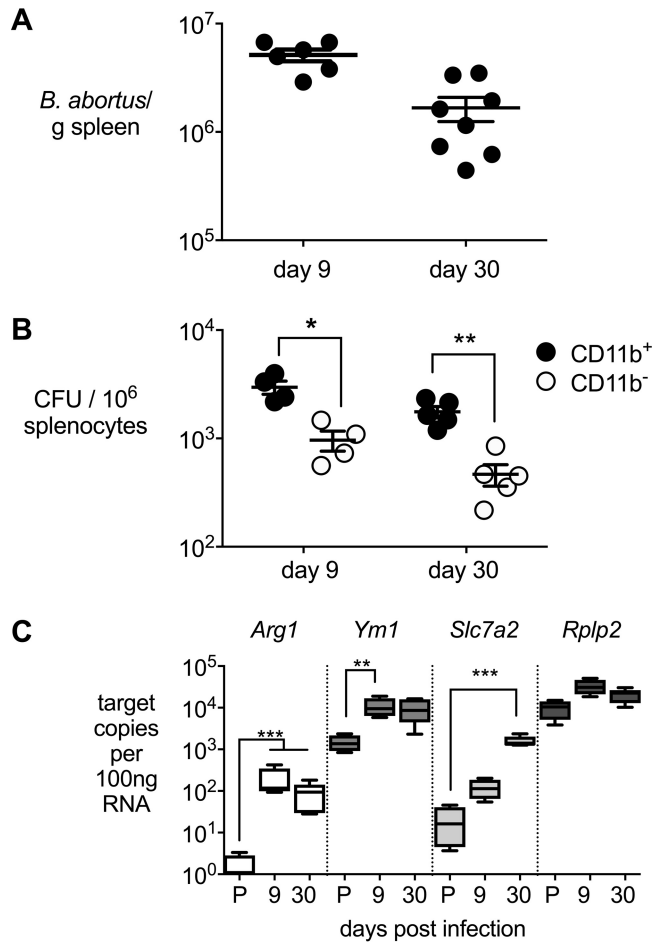


**FIG 2** *B. abortus* resides in CD11b<sup>+</sup> splenocytes that express features of alternative activated macrophages. (A) *B. abortus* 2308 CFU in spleens from i.p. infected BALB/c mice enumerated 9 ( $n = 6$ ) and 30 ( $n = 8$ ) days postinfection. (B) Bacterial counts of *B. abortus* 2308 in CD11b<sup>+</sup> and CD11b<sup>-</sup> splenocytes from BALB/c mice 9 ( $n = 4$ ) and 30 ( $n = 5$ ) days postinfection. (C) Absolute copy numbers of alternatively activated macrophage markers *Arg-1*, *Ym1*, and *Slc7a2* of CD11b<sup>+</sup> splenocytes from BALB/c mice infected with *B. abortus* 2308 or treated with D-PBS (Invitrogen) 9 days ( $n = 4$ ) and 30 days ( $n = 5$ ) postinfection. P, D-PBS; *Rplp2*, housekeeping control gene (encoding the large ribosomal subunit protein P2). Values represent means  $\pm$  standard errors of the means (SEM). For panel B, the significance of differences between experimental groups at a single time point was determined using an unpaired *t* test on log-transformed data. For panel C, the significance of differences between each infection time point and uninfected mice was determined using an unpaired *t* test on log-transformed data. \*,  $P < 0.05$ ; \*\*,  $P < 0.01$ ; \*\*\*,  $P < 0.005$ .

replication. The product of arginase-1, ornithine, can be decarboxylated by ornithine decarboxylase (ODC) into the polyamine putrescine. To determine whether uptake of putrescine by *B. abortus* contributes to its persistence in mice, we determined the effect of *potIHGF* inactivation on the fitness of *B. abortus* 30 days after i.p. infection of mice. The *potIHGF* mutant strain (TOK13) had a small but significant 3-fold competitive defect in the spleen compared to the parent strain at 30 days postinfection (Fig. 3C), suggesting that uptake of putrescine contributes to a higher pathogen burden in the spleen during chronic infection with *B. abortus*.

**Inhibition of arginase-1 leads to reduced intracellular availability of L-ornithine and putrescine.** To determine if *B. abortus* replication in IL-4 and IL-13 (IL-4+IL-13)-polarized macrophages depends on products of the arginase-1 pathway, we measured the intracellular concentrations of L-ornithine, an arginase-1 product, and of putrescine, a product of the downstream ODC reaction. Treatment of bone marrow-derived macrophages (BMMs) with IL-4+IL-13 led to an increase in cellular ornithine (Fig. 4A). The elevated levels of ornithine were reversed by inhibition of arginase-1 with nor-

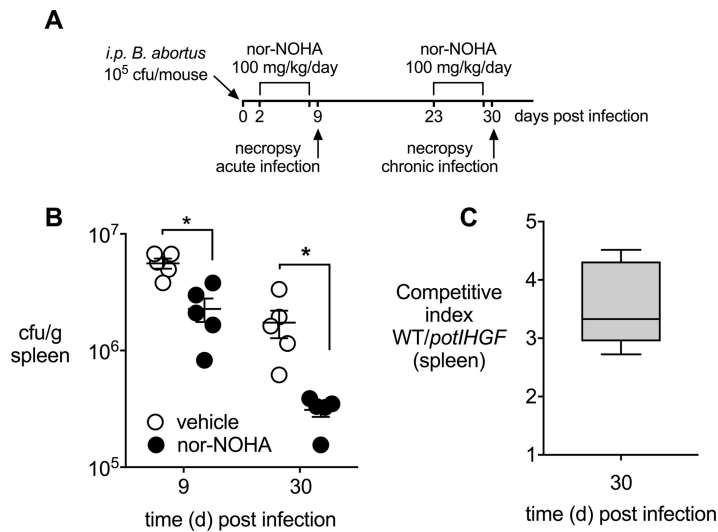


**FIG 3** Inhibition of arginase-1 activity reduces splenic *B. abortus* colonization. (A) Treatment regime to inhibit arginase-1 activity *in vivo* using 100 mg/kg/day nor-NOHA (Cayman Chemical, USA) for 6 consecutive days. (B) Survival of *B. abortus* 2308 in spleens from infected and nor-NOHA-treated BALB/cJ mice ( $n = 5$ ) compared to infected but vehicle control (D-PBS)-treated mice ( $n = 5$ ) at 6 and 30 days postinfection. (C) Competitive index, calculated for day 30 postinfection based on CFU from spleens of BALB/cJ mice infected with a 1:1 mixture of *B. abortus* 2308 and the *potIHGF* mutant. Values represent means  $\pm$  SEM. The statistical significance of differences between groups was determined using an unpaired *t* test analysis on log-transformed data. \*,  $P < 0.05$ .

NOHA (Fig. 4A) without significantly affecting the intracellular levels of other amino acids (Fig. 4B). Similar results were obtained when we measured intracellular putrescine concentrations by gas chromatography-mass spectrometry (GC-MS) (Fig. 4C), suggesting that inhibition of arginase-1 affects the abundance of polyamines that may promote intracellular replication of *B. abortus*. While treatment of macrophages with IFN- $\gamma$  can shift their energy metabolism toward anaerobic glycolysis, inhibition of arginase-1 with nor-NOHA did not have this effect, since production of lactate, the end product of anaerobic glycolysis, was unaffected (Fig. 4D). Inhibition of arginase-1 also did not increase macrophage production of NO, as measured by the Griess assay (Fig. 4E). These observations imply that inhibition of arginase-1 limits the availability of L-ornithine and putrescine without shifting the phenotype of macrophages to that of IFN- $\gamma$ -treated macrophages or inducing other pathways that could limit intracellular survival of *B. abortus*.

**Increased abundance of polyamines supports growth of *B. abortus* in IL-4+IL-13-treated macrophages.** The above-described observations in mice suggested a role for metabolites of the arginase-1 pathway in supporting chronic *B. abortus* infection, but since arginase-1 inhibition in the mouse could affect other cells in addition to macrophages, we asked whether IL-4+IL-13 treatment of macrophages promotes intracellular replication of *B. abortus* via increased availability of polyamines. To test this idea, BMMs from BALB/c mice were differentiated with IL-4+IL-13 and treated either with nor-NOHA or with the ODC inhibitor difluoromethylornithine (DFMO), which prevents production of putrescine (Fig. 5A). In addition, two control experiments were performed to assess the effects of the inhibitors on extracellular growth of *B. abortus* (Fig. 5B) and on uptake of bacteria by treated macrophages (Fig. 5C). While nor-NOHA and DFMO had no effect on *B. abortus* growth in TSB (Fig. 5B), treatment of IL-4+IL-13-treated J774 macrophages with either inhibitor increased uptake of *B. abortus* but blocked intracellular replication of the internalized bacteria compared to untreated cells (Fig. 5C). In BMMs, blockade of either arginase-1 or ODC also significantly reduced intracellular replication of *B. abortus*, suggesting that the arginase-1 pathway contributes significantly to intracellular replication of *B. abortus* within IL-4+IL-13-treated macrophages (Fig. 5D). We used IFN- $\gamma$ -treated macrophages as a control for a condition

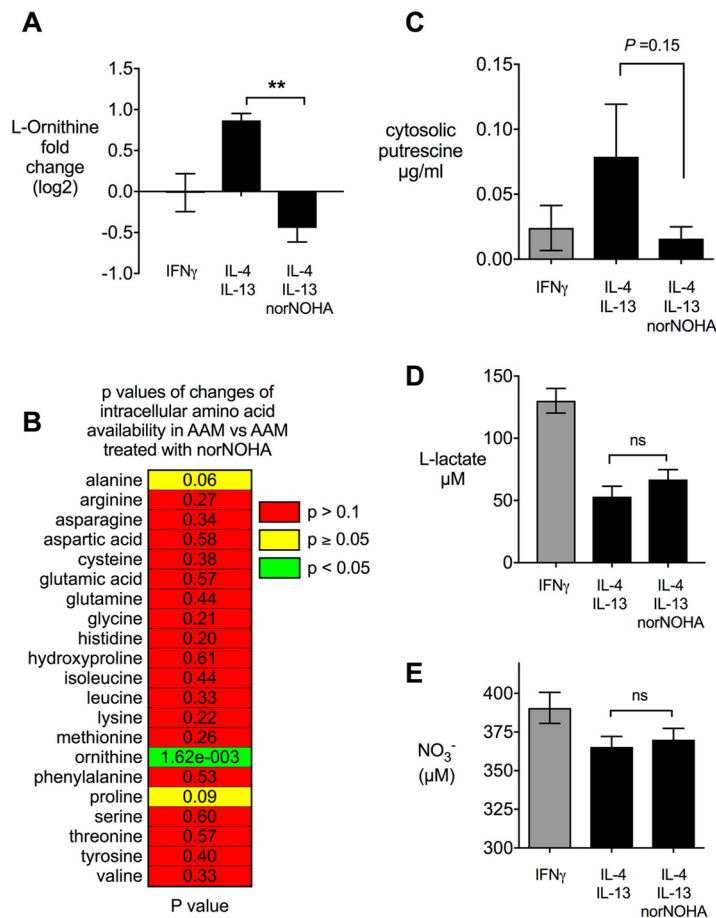


**FIG 4** Inhibition of arginase-1 in alternatively (IL-4+IL-13) activated macrophages leads to reduced intracellular availability of L-ornithine and putrescine without changing the activation state of the macrophages. (A) Intracellular L-ornithine levels measured in BMMs after treatment with inducers. (B) Influence of the arginase-1 inhibitor nor-NOHA on the amino acid pool in IL-4+IL-13-polarized macrophages. (C) Concentration of putrescine in IFN- $\gamma$ -polarized and IL-4+IL-13-polarized BMMs and effect of nor-NOHA treatment. (D and E) Effects of arginase-1 inhibition on production of lactate (D) and NO (E) by IL-4+IL-13-polarized macrophages. Results from IFN- $\gamma$ -polarized macrophages are shown as a reference. Values represent means  $\pm$  SEM. Differences between IL-4+IL-13-treated groups were analyzed using an unpaired *t* test analysis on log-transformed data. \*\*, *P* < 0.01; ns, not significant.

that restricts intracellular replication of *B. abortus*. Interestingly, the effect of inhibiting arginase-1 was similar to that of inactivating the putrescine uptake system encoded by *potIHGF*, suggesting putrescine as a potential nutrient that fuels replication within this population of macrophages.

**DISCUSSION**

*B. abortus* persists within the cells of the mononuclear phagocyte system to cause chronic infection. One niche for persisting bacteria is within macrophages expressing phenotypic markers of alternate activation (16). Considering the metabolic differences between classically (M1, IFN- $\gamma$ ) activated macrophages and other, less inflammatory macrophage populations, it is likely that the metabolism of *B. abortus* is adapted to take advantage of this niche by utilizing other metabolites that are more abundant in AAMs. Previous work has shown that glucose uptake in this niche supports the chronic stages of brucellosis (16, 28). To further define this important replicative niche especially during chronic *Brucella* infection, we investigated the role of polyamines, mainly putrescine, in the survival of *B. abortus* inside AAMs since it was described that the arginase-1-driven polyamine synthesis is considered to be a hallmark of M2 or AAMs (29).

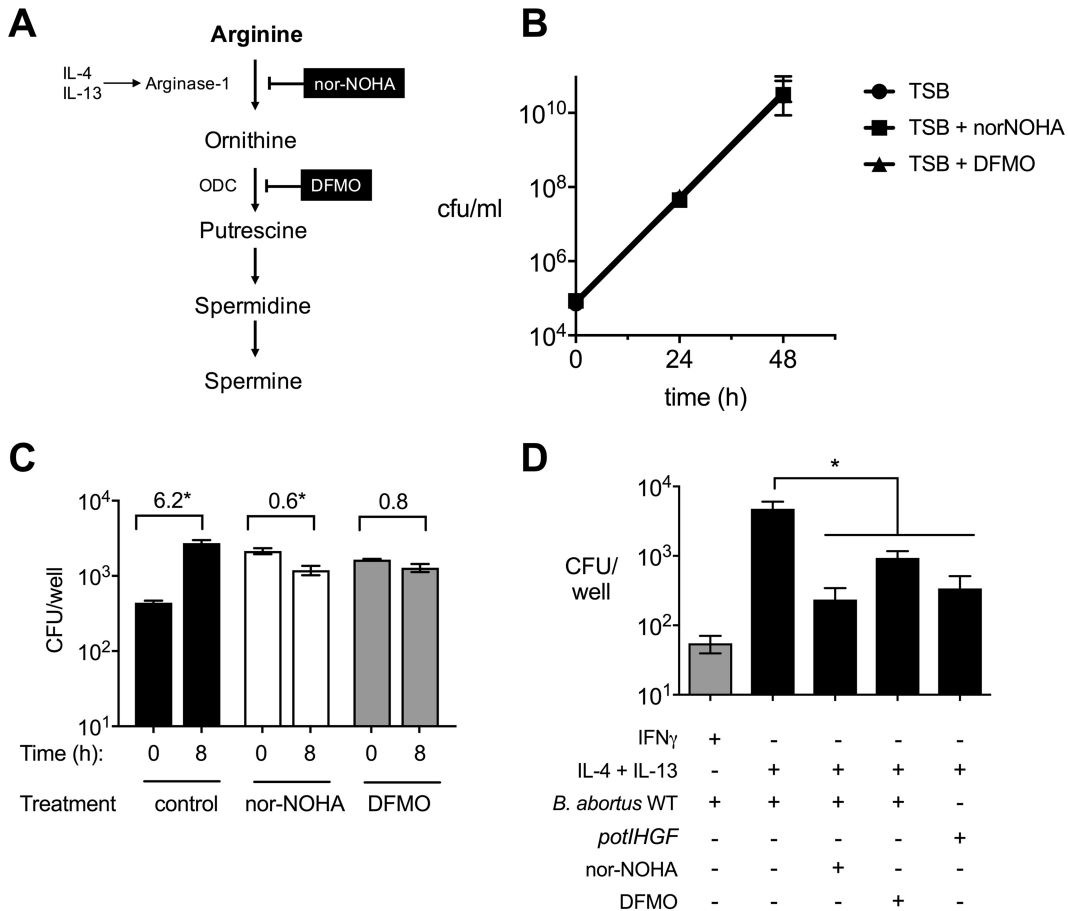


**FIG 5** Intracellular *de novo* synthesis of polyamines is beneficial for *B. abortus* replication in IL-4+IL-13-activated BMMs. (A) Simplified model of the polyamine synthesis pathway in macrophages treated with IL-4 and IL-13. Targets of the inhibitors nor-NOHA and DFMO are shown. ODC, ornithine decarboxylase. (B) Growth of *B. abortus* in TSB supplemented with inhibitors of arginase-1 (nor-NOHA) or ornithine decarboxylase (DFMO). (C) Effects of nor-NOHA and DFMO treatments on uptake and early replication of *B. abortus* in IL-4+IL-13-treated J774 macrophages. Numbers above each experimental group represent the fold increase in intracellular *B. abortus* between 0 h and 8 h. Asterisks represent significant differences between time points determined using Student's *t* test on logarithmically transformed data. (D) Intracellular survival of *B. abortus* 2308 WT and the *potIHGF* mutant at 48 h postinfection of BMMs. IFN- $\gamma$ -treated macrophages are shown as a reference. Values represent means  $\pm$  SEM. The statistical significance of differences between IL-4+IL-13-treated macrophages and macrophages treated with inhibitors or infected with the *potIHGF* mutant was determined using a one-way ANOVA with a Tukey's multiple-comparison test. Asterisks represent significant differences between groups ( $P < 0.05$ ).

Inhibition of host-derived putrescine production impaired the intracellular bacterial survival of *B. abortus ex vivo* in AAMs as well as *in vivo* in BALB/c mice. Further, a mutant in a locus encoding a predicted putrescine transporter, *potIHGF*, had a competitive fitness defect during chronic infection, suggesting that putrescine is a likely nutrient for *B. abortus* during this phase of infection. While no predicted bacterium-type ODC that could serve as a source of putrescine was identified in the *B. abortus* genome, the protein encoded by ORF BAB2\_0098 shares similarity with eukaryotic ODC (KEGG), suggesting that *B. abortus* might be able to produce putrescine under some conditions. However, if this is the case, it appears to be unable to compensate for the blockade of host-derived putrescine production in macrophages (Fig. 5C and D). It should also be noted that *potIHGF* is not the only predicted transporter gene for arginine metabolites in the *B. abortus* genome, as BAB2\_0876-0879 and BAB2\_1062-1064/BAB2\_1129 encode putative transporters for ornithine and putrescine/spermidine, respectively. Interestingly, the *Brucella melitensis* homolog of BAB2\_0876-0879 appears also to contribute to chronic infection (30), suggesting that *Brucella* spp. have multiple mechanisms for acquiring metabolites of the arginase-1 pathway *in vivo*.

Our observation that survival of *B. abortus* during chronic infection is promoted by arginase-1 activity is consistent with the findings of Hanot Mambres et al., who found that in IL-12p40<sup>-/-</sup> mice, which are defective in IFN- $\gamma$  production and express elevated levels of IL-4 (31), *B. abortus* was associated with cells expressing arginase-1 (26). In this previous study, *in situ* analysis showed that the arginase-expressing cells had features of dendritic cells, suggesting that in our *in vivo* experiments, inhibition of arginase-1 could affect other cell types in addition to macrophages. During its intracellular survival, access of *B. abortus* to polyamines such as putrescine can be explained by its route of intracellular trafficking. Polyamines have been localized within acidified compartments in the host cell that have features of late endocytic compartments (32). Upon phagocytic uptake, vacuoles containing *Brucella* mature along the endocytic pathway and fuse with lysosomes (21). After exclusion of lysosomal markers, *B. abortus* replicates within a compartment that is associated with the endoplasmic reticulum (21, 33). To complete its intracellular cycle and spread to the next cell, *B. abortus* subsequently subverts a subset of autophagy proteins to form a compartment that regains features of the endosome, including its acidified nature (34). Therefore, during at least two stages of its intracellular life cycle, *B. abortus* should be exposed to a polyamine-containing environment.

The contribution of polyamines to the survival of *B. abortus* in the host may shed light on the differing susceptibilities of specific genetic mouse backgrounds to *Brucella* infections. It is generally accepted that mice of the C57BL/6 genetic background are more resistant to *Brucella* infections than are BALB/c mice (35), with a difference of about 1 order of magnitude in splenic colonization levels after i.p. inoculation. In contrast to what is observed in BALB/c mice, the enhanced clearance of *Brucella* in C57BL/6 mice was attributed to the expression of the proinflammatory cytokine IFN- $\gamma$  during the acute phase of the infection, which further translated to the diminished ability of *Brucella* to establish chronic infections (36). The less-permissive C57BL/6 mice produce the proinflammatory cytokine IFN- $\gamma$ , which shifts the balance in the macrophage pool toward classic or M1 activation and thus would be expected to contain lower levels of intracellular polyamines as a nutrient source for *Brucella*. In contrast, the macrophages of BALB/c mice, which have a reduced and delayed expression of IFN- $\gamma$  during infection, expressed markers of alternative activation earlier during infection than what was previously described for C57BL/6 mice (16). These findings are consistent with a report on *Leishmania* infection showing that macrophages from C57BL/6 mice have impaired arginine uptake as a result of a mutation in the promoter of the arginine solute carrier SLC7a2 (25). Expression of this solute carrier is induced by IL-4+IL-13 and is essential to import sufficient arginine for arginase-1 activity and downstream polyamine production. These polyamines can then be exploited by *B. abortus* as a nutrient source to promote the intracellular chronicity of the pathogen. In conclusion, our results show that products of the arginase-1/polyamine pathway in IL-4+IL-13-activated macrophages support intracellular replication and chronic infection by *B. abortus*. This finding identifies this pathway as a potential target for strategies to limit or eradicate chronic infection, an idea that merits further investigation.

## MATERIALS AND METHODS

**Bacterial strains, media, and culture conditions.** *Brucella abortus* 2308 was used as the wild-type strain for this work. All work with live *B. abortus* was performed at biosafety level 3 and was approved by the Institutional Biosafety Committee at the University of California, Davis. To generate the putrescine uptake-negative *potIHGF* mutant strain (TOK13), we inserted the plasmid pTK411 by homologous recombination to disrupt the operon encoding the *potIHGF* locus in *B. abortus* 2308. The plasmid pTK411 is a pBlueScript II SK(+)-based plasmid carrying two amplified 500-bp fragments flanking the *potIHGF* operon using the primer combinations (i) pBI-KS-3-A-Fwd (5'-gcggtggcggcgcctGACCGGCATCGGCTACAA-3') and H2-0414-Rev (5'-ccagttgttCGAATAGCCGATCTCCACC-3') for fragment H1-0411-A and (ii) H1-0411-Fwd (5'-gctattcgAACAACTGGTCCCGCTTC-3') and pBI-KS-3-B-Rev (5'-ggccccctcgaggGGTCGAAATTCA TCGCCAC-3') for fragment H2-0414-B (where lowercase bases represent overlapping regions for Gibson assembly of the plasmid). The fragments were fused together and cloned into the vector backbone by using the Gibson cloning (NEB, USA). Successful cloning steps were verified by PCR and sequencing. The resulting construct, designated pTK411t, was introduced into *B. abortus* 2308 by electroporation, and ampicillin resistance was used to identify recombinants. The phenotype of the *potIHGF* mutant was



confirmed by loss of growth promotion by putrescine in modified F-12/K medium. Strains were cultured on tryptic soy agar (TSA; Difco/Becton Dickinson, Sparks, MD) or tryptic soy broth at 37°C on a rotary shaker. For mouse infection, bacteria were cultured on TSA plates containing 5% sheep blood for 3 days. Ampicillin (250 mg/ml) or kanamycin (100 mg/ml) was added to the culture media to select resistant *B. abortus* strains. To address the importance of putrescine to growth of *B. abortus in vitro*, we formulated a modified version (modified F-12/K; see Table S1 in the supplemental material) of the commercially available F-12/K medium (Invitrogen, USA) according to the manufacturer's formulation, which included all inorganic salts, D-glucose, hypoxanthine Na, lipoic acid, sodium pyruvate, and thymidine, with the addition of minimum essential medium (MEM) amino acids solution (50×) liquid and MEM vitamin solution (100×) liquid (both from Invitrogen, USA) to complete the medium. When needed, putrescine (Santa Cruz Biotechnology, USA) was added at the manufacturer's suggested concentration of 0.32 mg/liter.

To investigate the contribution of putrescine uptake to growth of *B. abortus* 2308 and of the *potIHGF* mutant strain (TOK13) *in vitro*, bacterial pellets of fresh overnight cultures were washed three times with sterile Dulbecco's phosphate-buffered saline (D-PBS; Invitrogen) and suspended in modified F-12/K with and without putrescine at  $0.5 \times 10^5$  to  $1 \times 10^5$  CFU/ml. Bacterial cultures (5 ml) were incubated for 24 h at 37°C in 50-ml conical tubes with tightly closed lids on a rotary shaker. Serial dilutions of the bacterial culture in sterile PBS were plated to enumerate CFU/ml and to calculate bacterial growth over a 24-h period.

**Animal experiments.** Female BALB/cJ mice obtained from the Jackson Laboratory (USA) were used for this study. Mice were held in individually ventilated microisolator cages (Tecniplast, West Chester, PA) with sterile bedding and irradiated feed in a biosafety level 3 laboratory. All animal experiments were approved by the University of California Laboratory Animal Care and Use Committee and were conducted in accordance with institutional guidelines. Groups of four to six mice were inoculated intraperitoneally (i.p.) with 0.1 ml of PBS containing  $1 \times 10^5$  CFU of *B. abortus* 2308 or a 1:1 mixture of *B. abortus* 2308 and the *potIHGF* mutant as previously described (37). When needed, mice were treated daily for 7 days with i.p. injection of 100 mg/kg of body weight/day of the arginase inhibitor nor-NOHA (Cayman Chemical, USA) diluted in 0.1 ml of sterile D-PBS. Sterile D-PBS was used as a vehicle control. At various time points after infection, mice were euthanized via CO<sub>2</sub> inhalation, and spleens and serum from the animals were collected aseptically at necropsy. Spleens were weighed and homogenized in 4 ml of PBS to enumerate CFU per organ using serial dilutions of the homogenate plated on TSA alone or TSA with ampicillin (250 ng/ml). Spleen samples were also collected for gene expression, flow cytometry, and immunohistochemistry analysis.

**BMM infection.** BMMs were differentiated as previously described by Murray et al. (29) and Rolan et al. (37) from femora and tibiae of female 6- to 8-week-old BALB/c mice. To determine the contribution of *de novo* polyamine synthesis to the cellular survival of *B. abortus* strains, BMMs were maintained in RPMI 1640 medium supplemented with 10% heat-inactivated and dialyzed (3,500 molecular weight cutoff [MWCO]) fetal calf serum (FCS), 0.03% L-glutamine, 1 mM nonessential amino acids, 1 mM sodium pyruvate (all from Invitrogen, USA) according to the method of Van den Bossche et al. (38). For infection of BMMs with different *B. abortus* strains, 24-well microtiter plates were seeded with  $5 \times 10^5$  macrophages per well in 0.5 ml of medium and incubated for 48 h at 37°C in 5% CO<sub>2</sub>. Bacterial inoculation and infection of BMMs were done using a gentamicin protection assay as described in reference 16 with a multiplicity of infection (MOI) of 100 in RPMI that was formulated as described above. Bacterial survival was enumerated by plating serial dilutions on TSA or on TSA plus ampicillin (250 µg/ml) 48 h after infection using BMMs that were lysed with 0.5 ml of 0.5% Tween 20. For purification of proteins and RNA, BMMs were directly resuspended in 0.5 ml of TRIzol (Invitrogen, USA) and stored at -80°C until further use. To block *de novo* synthesis of polyamines, the specific arginase inhibitors nor-NOHA (Cayman Chemicals, USA) and DFMO (Sigma) to block ornithine decarboxylase were used according to the recommendation of Van den Bossche et al. (38). To induce classical activation of BMMs (CAMs), 10 ng/ml of mouse recombinant IFN-γ (rIFN-γ; BD Bioscience, San Jose, CA) was used. AAMs were generated using 10 ng/ml of mouse rIL-4 (mrIL-4; R&D Systems, USA) and 5 ng/ml rIL-13 (R&D Systems, USA). All treatments were added to the cells either 48 h (nor-NOHA, DFMO) or 24 h (mrIL-4/-13) prior to experiments and maintained throughout the experiments. Experiments were performed independently in duplicate at least four times, and the standard error for each time point was calculated. To control for any effect of treatments on macrophage viability, lactate dehydrogenase (LDH) release was assayed using the CytoTox 96 nonradioactive cytotoxicity (Promega). At the concentrations used, no significant difference in LDH release was observed between groups treated with IFN-γ, IL-4/IL-13, DFMO, or NOHA and untreated controls (data not shown).

**CD11b<sup>+</sup> cell isolation.** Macrophages (CD11b<sup>+</sup> cells) were isolated from the spleens of *B. abortus*-infected BALB/cJ mice using a MACS CD11b MicroBeads magnetic cell sorting kit from Miltenyi Biotech (Auburn, CA) according to the manufacturer's instructions as previously described (39). To enumerate viable *B. abortus* in CD11b<sup>-</sup> and CD11b<sup>+</sup> splenocyte fractions, 10-fold serial dilutions of each fraction in sterile PBS were plated on TSA plates and the numbers of viable bacteria were normalized to CFU per 10<sup>6</sup> splenocytes.

**Gene expression analysis.** Eukaryotic gene expression was determined by quantitative real-time PCR (qRT-PCR) as previously described (40). RNA was isolated using TRIzol (Invitrogen, USA) according to the manufacturer's instructions. To synthesize cDNA, a reverse transcriptase reaction was performed using 500 ng of total RNA, random hexamers (Applied Biosystems, USA), and TaqMan reverse transcription reagents (Applied Biosystems, Carlsbad, CA). Real-time PCR was performed using SYBR green (Applied Biosystems) with the primers listed in Table S2 in the supplemental material. Absolute copy

numbers for *Arg1*, *Ym1*, and *Slc7a2* were calculated based on individually cloned plasmid standards and were normalized to 100 ng input RNA used for the cDNA synthesis. The housekeeping gene *Rplp2*, encoding the large ribosomal protein 2, was included as a control.

**Intracellular amino acid content measurement.** Measurement of total intracellular amino acid contents of differentially activated and/or nor-NOHA-treated BALB/c BMMs was performed by the UC Davis Genome Center Proteomics core. For sample preparation, BMMs treated for 48 h were intensively washed 4 times with sterile D-PBS (Invitrogen, USA). Three wells of a 6-well plate were combined in a total of 1 ml of sterile PBS, and cells were detached by scraping. All samples were stored at  $-80^{\circ}\text{C}$  until further use. For amino acid analysis, 50  $\mu\text{l}$  of 10% sulfosalicylic acid (Sigma-Aldrich, USA) was added to 200  $\mu\text{l}$  of sample and mixed at room temperature for 15 min, and the mixture was stored overnight at  $-20^{\circ}\text{C}$ . The thawed samples were vortexed and centrifuged, and 100  $\mu\text{l}$  of supernatant was spiked with 3.75 nmol AE-Cys as an internal standard. The amount of free amino acids was analyzed using the Hitachi L-8900 amino acid analyzer.

**Intracellular putrescine measurements by GC-MS.** Intracellular levels of the polyamine putrescine were measured according to the protocol for sample preparation, derivatization chemistry, and GC-MS conditions that was previously published by Chen et al. (41, 42). BMMs were cultured as described for the amino acid analysis, and 2 wells of a 6-well culture plate were combined and detached by scraping in 1 ml of 10% NaCl (pH = 10) according to the method of Chen et al. (42). One microgram of Put- $\text{D}_8$  (CDN Isotopes, Canada) was used as an internal standard. A TQ8040 GC-MS/MS instrument (Shimadzu) was employed to detect intracellular levels of putrescine in differentially activated bone marrow-derived macrophages. All mass spectra were acquired in electron ionization (EI) for all measurements in the selected-ion monitoring (SIM) mode for putrescine- $\text{d}_8$  and the multiple-reaction monitoring (MRM) mode for putrescine. Helium carrier gas was set to a column head pressure of 149.5 kPa at a flow rate of 1.75 ml/min. Sample aliquots of 2  $\mu\text{l}$  were injected with a split ratio of 5 with a 5-min solvent delay. GC analyses were done with an Rtx-5Sil MS capillary column (30-m length, 0.25-mm inner diameter [i.d.], and 0.25- $\mu\text{m}$  thickness; Restek, USA) programmed from  $140^{\circ}\text{C}$  to  $210^{\circ}\text{C}$  at  $8^{\circ}\text{C}/\text{min}$ , followed by a 2-min hold, and then to  $300^{\circ}\text{C}$  at  $20^{\circ}\text{C}/\text{min}$ , followed by a 4-min hold. A final temperature increase to  $320^{\circ}\text{C}$  at  $20^{\circ}\text{C}/\text{min}$  was held as bake out for 4 min. MS conditions were the following: source,  $200^{\circ}\text{C}$ ; interface,  $300^{\circ}\text{C}$ ; injector,  $260^{\circ}\text{C}$ ; electron energy, 70 eV; typical source pressure,  $1.8 \times 10^{-5}$  torr. Full scans were over the mass range  $m/z$  10 to 700 at 2.0 scans/s for the SIM mode. A total of 3 ions from putrescine and its fragmentation products were used to monitor Put. SIM and full-scan acquisitions were started at 5.20 min and ended at 17.73 min. The first ion group consisted of three ions with  $m/z$  166, 283, and 355 for putrescine- $\text{d}_8$  running for 5 to 8 min with a dwell time of 100 ms. Detection and quantification of the abundance of the internal standard putrescine by MRM was done using the ions  $283 > 142$   $m/z$  and  $355 > 211$  in the above-mentioned time frame. While all ions in each group were monitored for peak verification, the ions used for quantification were those in italics above. Instrument run, peak measurements, and data analysis were done with the GCMS solution software (Shimadzu, USA). To normalize the data, we used the detected concentration of the putrescine- $\text{d}_8$  in each individual sample as a calibrator to calculate a factor that normalizes all samples to the same putrescine- $\text{d}_8$  level as the one that was detected in the untreated BMM within each mouse. These factors were multiplied with the detected putrescine areas for each sample based on the corresponding individual calibration factor calculated for each sample in each mouse to normalize the data. Prism (GraphPad, USA) was used to graph the normalized areas and to compute statistical analysis based on the log of normalized areas using a paired, one-tailed Student's *t* test.

**Metabolite measurements.** For determination of secreted L-lactate levels, BALB/c BMMs were grown in 24-well plates and infected as described above. At 24 and 48 h postinfection, the cell culture supernatant was harvested and deproteinized using perchloric acid (Abcam, USA). L-lactate was measured using the L-lactate assay kit II (Eton Bioscience, USA). To follow the production of reactive nitrogen species by macrophages *ex vivo*, we measured the levels of nitrate and nitrite in cell culture supernatants of activated and infected macrophages 48 h postinfection using an adaptation of the Griess assay as described by Lopez et al. (43).

**Statistical analysis.** Fold changes of ratios (bacterial numbers or mRNA levels) and percentages (flow cytometry and fluorescence microscopy) were transformed logarithmically prior to statistical analysis. An unpaired Student's *t* test was used on the transformed data to determine whether differences between groups were statistically significant ( $P < 0.05$ ). When more than two treatments were used, statistically significant differences between groups were determined by an ordinary one-way analysis of variance (ANOVA) and the Sidak test for multiple comparisons. All statistical analyses were performed using GraphPad Prism software (GraphPad Software, USA).

## SUPPLEMENTAL MATERIAL

Supplemental material for this article may be found at <https://doi.org/10.1128/IAI.00458-17>.

**SUPPLEMENTAL FILE 1**, PDF file, 0.1 MB.

## ACKNOWLEDGMENTS

This work was supported by PHS grants AI112258 and AI109799 to R.M.T. and AI118807 and AI128151 to S.E.W. Work in S.E.W.'s laboratory is supported by a grant from the Welch Foundation (I-1858).

## REFERENCES

- Antoine JC, Prina E, Jouanne C, Bongrand P. 1990. Parasitophorous vacuoles of *Leishmania amazonensis*-infected macrophages maintain an acidic pH. *Infect Immun* 58:779–787.
- Weiss G, Schaible UE. 2015. Macrophage defense mechanisms against intracellular bacteria. *Immunol Rev* 264:182–203. <https://doi.org/10.1111/imr.12266>.
- Ruby T, McLaughlin L, Gopinath S, Monack D. 2012. *Salmonella*'s long-term relationship with its host. *FEMS Microbiol Rev* 36:600–615. <https://doi.org/10.1111/j.1574-6976.2012.00332.x>.
- Byndloss MX, Tsois RM. 2016. Chronic bacterial pathogens: mechanisms of persistence. *Microbiol Spectr* 4(2). <https://doi.org/10.1128/microbiolspec.VMBF-0020-2015>.
- Byndloss MX, Tsois RM. 2016. *Brucella* spp. virulence factors and immunity. *Annu Rev Anim Biosci* 4:111–127. <https://doi.org/10.1146/annurev-animal-021815-111326>.
- Scott P, Novais FO. 2016. Cutaneous leishmaniasis: immune responses in protection and pathogenesis. *Nat Rev Immunol* 16:581–592. <https://doi.org/10.1038/nri.2016.72>.
- Tan S, Russell DG. 2015. Trans-species communication in the *Mycobacterium tuberculosis*-infected macrophage. *Immunol Rev* 264:233–248. <https://doi.org/10.1111/imr.12254>.
- Van Dyken SJ, Locksley RM. 2013. Interleukin-4- and interleukin-13-mediated alternatively activated macrophages: roles in homeostasis and disease. *Annu Rev Immunol* 31:317–343. <https://doi.org/10.1146/annurev-immunol-032712-095906>.
- Gordon S, Martinez FO. 2010. Alternative activation of macrophages: mechanism and functions. *Immunity* 32:593–604. <https://doi.org/10.1016/j.immuni.2010.05.007>.
- Shi C, Pamer EG. 2011. Monocyte recruitment during infection and inflammation. *Nat Rev Immunol* 11:762–774. <https://doi.org/10.1038/nri3070>.
- Reyes JL, Terrazas LI. 2007. The divergent roles of alternatively activated macrophages in helminthic infections. *Parasite Immunol* 29:609–619. <https://doi.org/10.1111/j.1365-3024.2007.00973.x>.
- Shirey KA, Cole LE, Keegan AD, Vogel SN. 2008. *Francisella tularensis* live vaccine strain induces macrophage alternative activation as a survival mechanism. *J Immunol* 181:4159–4167. <https://doi.org/10.4049/jimmunol.181.6.4159>.
- Lawrence T, Natoli G. 2011. Transcriptional regulation of macrophage polarization: enabling diversity with identity. *Nat Rev Immunol* 11:750–761. <https://doi.org/10.1038/nri3088>.
- Chawla A. 2010. Control of macrophage activation and function by PPARs. *Circ Res* 106:1559–1569. <https://doi.org/10.1161/CIRCRESAHA.110.216523>.
- Odegaard JI, Ricardo-Gonzalez RR, Goforth MH, Morel CR, Subramanian V, Mukundan L, Red Eagle A, Vats D, Brombacher F, Ferrante AW, Chawla A. 2007. Macrophage-specific PPARgamma controls alternative activation and improves insulin resistance. *Nature* 447:1116–1120. <https://doi.org/10.1038/nature05894>.
- Xavier MN, Winter MG, Spees AM, den Hartigh AB, Nguyen K, Roux CM, Silva TM, Atluri VL, Kerrinnes T, Keestra AM, Monack DM, Luciw PA, Eigenheer RA, Baumler AJ, Santos RL, Tsois RM. 2013. PPARgamma-mediated increase in glucose availability sustains chronic *Brucella abortus* infection in alternatively activated macrophages. *Cell Host Microbe* 14:159–170. <https://doi.org/10.1016/j.chom.2013.07.009>.
- Eisele NA, Ruby T, Jacobson A, Manzanillo PS, Cox JS, Lam L, Mukundan L, Chawla A, Monack DM. 2013. *Salmonella* require the fatty acid regulator PPARdelta for the establishment of a metabolic environment essential for long-term persistence. *Cell Host Microbe* 14:171–182. <https://doi.org/10.1016/j.chom.2013.07.010>.
- Corraliza IM, Soler G, Eichmann K, Modolell M. 1995. Arginase induction by suppressors of nitric oxide synthesis (IL-4, IL-10 and PGE2) in murine bone-marrow-derived macrophages. *Biochem Biophys Res Commun* 206:667–673. <https://doi.org/10.1006/bbrc.1995.1094>.
- Iniesta V, Gomez-Nieto LC, Corraliza I. 2001. The inhibition of arginase by N(omega)-hydroxy-L-arginine controls the growth of *Leishmania* inside macrophages. *J Exp Med* 193:777–784. <https://doi.org/10.1084/jem.193.6.777>.
- Gorvel JP, Moreno E. 2002. *Brucella* intracellular life: from invasion to intracellular replication. *Vet Microbiol* 90:281–297. [https://doi.org/10.1016/S0378-1135\(02\)00214-6](https://doi.org/10.1016/S0378-1135(02)00214-6).
- Starr T, Ng TW, Wehrly TD, Knodler LA, Celli J. 2008. *Brucella* intracellular replication requires trafficking through the late endosomal/lysosomal compartment. *Traffic* 9:678–694. <https://doi.org/10.1111/j.1600-0854.2008.00718.x>.
- Chain PS, Comerci DJ, Tolmasky ME, Larimer FW, Malfatti SA, Vergez LM, Aguero F, Land ML, Ugalde RA, Garcia E. 2005. Whole-genome analyses of speciation events in pathogenic bruceellae. *Infect Immun* 73:8353–8361. <https://doi.org/10.1128/IAI.73.12.8353-8361.2005>.
- Suzuki H, Kurihara S. 2015. Polyamine catabolism in prokaryotes. In Kusano T, Suzuki H (ed), *Polyamines*. Springer, Tokyo, Japan.
- Terui Y, Saroj SD, Sakamoto A, Yoshida T, Higashi K, Kurihara S, Suzuki H, Toida T, Kashiwagi K, Igarashi K. 2014. Properties of putrescine uptake by PotFGHI and PuuP and their physiological significance in *Escherichia coli*. *Amino Acids* 46:661–670. <https://doi.org/10.1007/s00726-013-1517-x>.
- Sans-Fons MG, Yeramian A, Pereira-Lopes S, Santamaria-Babi LF, Modolell M, Lloberas J, Celada A. 2013. Arginine transport is impaired in C57Bl/6 mouse macrophages as a result of a deletion in the promoter of Slc7a2 (CAT2), and susceptibility to *Leishmania* infection is reduced. *J Infect Dis* 207:1684–1693. <https://doi.org/10.1093/infdis/jit084>.
- Hanot Mambres D, Machelart A, Vandervinden JM, De Trez C, Ryffel B, Letesson JJ, Muraille E. 2015. In situ characterization of splenic *Brucella melitensis* reservoir cells during the chronic phase of infection in susceptible mice. *PLoS One* 10:e0137835. <https://doi.org/10.1371/journal.pone.0137835>.
- Tenu JP, Lepoivre M, Moali C, Brollo M, Mansuy D, Boucher JL. 1999. Effects of the new arginase inhibitor N(omega)-hydroxy-nor-L-arginine on NO synthase activity in murine macrophages. *Nitric Oxide* 3:427–438. <https://doi.org/10.1006/niox.1999.0255>.
- Hong PC, Tsois RM, Ficht TA. 2000. Identification of genes required for chronic persistence of *Brucella abortus* in mice. *Infect Immun* 68:4102–4107. <https://doi.org/10.1128/IAI.68.7.4102-4107.2000>.
- Murray PJ, Allen JE, Biswas SK, Fisher EA, Gilroy DW, Goerdts S, Gordon S, Hamilton JA, Ivashkiv LB, Lawrence T, Locati M, Mantovani A, Martinez FO, Mege JL, Mosser DM, Natoli G, Saeij JP, Schultze JL, Shirey KA, Sica A, Suttles J, Udalova I, van Genderachter JA, Vogel SN, Wynn TA. 2014. Macrophage activation and polarization: nomenclature and experimental guidelines. *Immunity* 41:14–20. <https://doi.org/10.1016/j.immuni.2014.06.008>.
- Ronneau S, Moussa S, Barbier T, Conde-Alvarez R, Zuniga-Ripa A, Moriyon I, Letesson JJ. 2016. *Brucella*, nitrogen and virulence. *Crit Rev Microbiol* 42:507–525. <https://doi.org/10.3109/1040841X.2014.962480>.
- Magram J, Connaughton SE, Warrior RR, Carvajal DM, Wu CY, Ferrante J, Stewart C, Sarmiento U, Faherty DA, Gately MK. 1996. IL-12-deficient mice are defective in IFN gamma production and type 1 cytokine responses. *Immunity* 4:471–481. [https://doi.org/10.1016/S1074-7613\(00\)80413-6](https://doi.org/10.1016/S1074-7613(00)80413-6).
- Soulet D, Gagnon B, Rivest S, Audette M, Poulin R. 2004. A fluorescent probe of polyamine transport accumulates into intracellular acidic vesicles via a two-step mechanism. *J Biol Chem* 279:49355–49366. <https://doi.org/10.1074/jbc.M401287200>.
- Celli J, Salcedo SP, Gorvel JP. 2005. *Brucella* coopts the small GTPase Sar1 for intracellular replication. *Proc Natl Acad Sci U S A* 102:1673–1678. <https://doi.org/10.1073/pnas.0406873102>.
- Starr T, Child R, Wehrly TD, Hansen B, Hwang S, Lopez-Otin C, Virgin HW, Celli J. 2012. Selective subversion of autophagy complexes facilitates completion of the *Brucella* intracellular cycle. *Cell Host Microbe* 11:33–45. <https://doi.org/10.1016/j.chom.2011.12.002>.
- Grillo M-J, Blasco J-M, Gorvel J-P, Moriyon I, Moreno E. 2012. What have we learned from brucellosis in the mouse model? *Vet Res* 43:29. <https://doi.org/10.1186/1297-9716-43-29>.
- Murphy EA, Sathiyaseelan J, Parent MA, Zou B, Baldwin CL. 2001. Interferon-gamma is crucial for surviving a *Brucella abortus* infection in both resistant C57BL/6 and susceptible BALB/c mice. *Immunology* 103:511–518. <https://doi.org/10.1046/j.1365-2567.2001.01258.x>.
- Rolan HG, Tsois RM. 2008. Inactivation of the type IV secretion system reduces the Th1 polarization of the immune response to *Brucella abortus* infection. *Infect Immun* 76:3207–3213. <https://doi.org/10.1128/IAI.00203-08>.
- Van den Bossche J, Lamers WH, Koehler ES, Geuns JMC, Alhonen L, Uimari A, Pirnes-Karhu S, Van Overmeire E, Morias Y, Brys L, Vereecke L, De Baetselier P, Van Genderachter JA. 2012. Pivotal advance: arginase-

- 1-independent polyamine production stimulates the expression of IL-4-induced alternatively activated macrophage markers while inhibiting LPS-induced expression of inflammatory genes. *J Leukoc Biol* 91: 685–699. <https://doi.org/10.1189/jlb.0911453>.
39. Rolan HG, Xavier MN, Santos RL, Tsolis RM. 2009. Natural antibody contributes to host defense against an attenuated *Brucella abortus virB* mutant. *Infect Immun* 77:3004–3013. <https://doi.org/10.1128/IAI.01114-08>.
40. Rolán HG, Tsolis RM. 2007. Mice lacking components of adaptive immunity show increased *Brucella abortus virB* mutant colonization. *Infect Immun* 75:2965–2973. <https://doi.org/10.1128/IAI.01896-06>.
41. Chen GG, Fiori LM, Mamer OA, Turecki G. 2011. High-resolution capillary gas chromatography in combination with mass spectrometry for quantification of three major polyamines in postmortem brain cortex. *Methods Mol Biol* 720:427–436. [https://doi.org/10.1007/978-1-61779-034-8\\_27](https://doi.org/10.1007/978-1-61779-034-8_27).
42. Chen GG, Turecki G, Mamer OA. 2009. A quantitative GC-MS method for three major polyamines in postmortem brain cortex. *J Mass Spectrom* 44:1203–1210. <https://doi.org/10.1002/jms.1597>.
43. Lopez CA, Rivera-Chavez F, Byndloss MX, Baumler AJ. 2015. The periplasmic nitrate reductase NapABC supports luminal growth of *Salmonella enterica* serovar Typhimurium during colitis. *Infect Immun* 83:3470–3478. <https://doi.org/10.1128/IAI.00351-15>.
44. Kusano T, Suzuki H. 2015. Polyamines: a universal molecular nexus for growth, survival, and specialized metabolism. Springer, Tokyo, Japan.
45. Caspi R, Billington R, Ferrer L, Foerster H, Fulcher CA, Keseler IM, Kothari A, Krummenacker M, Latendresse M, Mueller LA, Ong Q, Paley S, Subhraveti P, Weaver DS, Karp PD. 2016. The MetaCyc database of metabolic pathways and enzymes and the BioCyc collection of pathway/genome databases. *Nucleic Acids Res* 44:D471–D480. <https://doi.org/10.1093/nar/gkv1164>.
46. Kanehisa M, Goto S. 2000. KEGG: Kyoto encyclopedia of genes and genomes. *Nucleic Acids Res* 28:27–30. <https://doi.org/10.1093/nar/28.1.27>.